RESEARCH ARTICLE SUMMARY

NEUROBIOLOGY

Loss of a mammalian circular RNA locus causes miRNA deregulation and affects brain function

Monika Piwecka,* Petar Glažar,* Luis R. Hernandez-Miranda,* Sebastian Memczak, Susanne A. Wolf, Agnieszka Rybak-Wolf, Andrei Filipchyk, Filippos Klironomos, Cledi Alicia Cerda Jara, Pascal Fenske, Thorsten Trimbuch, Vera Zywitza, Mireya Plass, Luisa Schreyer, Salah Ayoub, Christine Kocks, Ralf Kühn, Christian Rosenmund, Carmen Birchmeier, Nikolaus Rajewsky†

INTRODUCTION: Recently, a special class of RNAs has excited researchers and triggered hundreds of now-published studies. Known as circular RNAs (circRNAs), these RNAs are produced by regular transcription from genomic DNA, but the two ends of the (usually) exonic transcripts are covalently closed, probably in most cases by noncanonical splice reactions. Most circRNAs are expressed in the cytoplasm and are unusually stable, suggesting that they may have functions that diverge from those of canonical messenger RNAs (mRNAs) or long noncoding RNAs (lncRNAs).

CircRNAs tend to be weakly expressed, but there are exceptions in animal brains. For example, in the mouse brain, a few hundred circRNAs are highly expressed, often with developmentally specific expression patterns that are conserved in the human brain. We previously proposed that circRNAs may, at least sometimes, serve as regulatory RNAs. A circRNA discovered by the Kjems laboratory, CDR1as, caught our attention because it was covered with >70 binding sites for the microRNA (miRNA) miR-7. Our data suggested that CDR1as might serve to alter the free concentration of miR-7. But what really is the function of CDR1as?

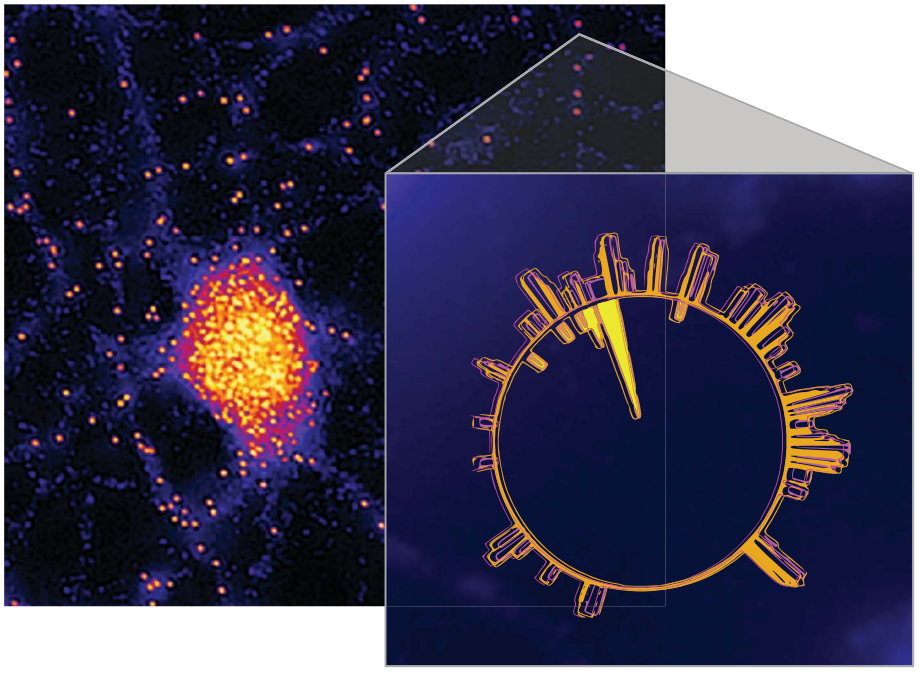

Cdr1as is a brain-enriched circular RNA, expressed in hundreds of copies within neurons and essential for maintaining normal brain function. Genetic ablation of the *Cdr1as* locus in mice led to deregulation of miR-7 and miR-671 in the brain, up-regulation of immediate early genes, synaptic malfunctions, and a deficit in prepulse inhibition of the startle reflex, a behavioral phenotype associated with neuropsychiatric disorders.

RATIONALE: We first determined which miRNAs specifically bind Cdr1as in postmortem human and mouse brains and characterized Cdr1as expression patterns. Once we had that information, we removed Cdr1as from the mouse genome to study the molecular and behavioral consequences.

RESULTS: We show that Cdr1as is, in the human brain, directly and massively bound by miR-7 and miR-671. In fact, Cdr1as is one of the most common transcripts targeted by miRNAs out of all brain mRNAs or lncRNAs. The expression of miRNAs was generally unperturbed in *Cdr1as* knockout (KO) mice, with the exception of the two miRNAs that directly interact with Cdr1as, miR-7 and miR-671, which were respectively down-regulated and up-regulated. This perturbation was post-transcriptional, consistent with a model in which Cdr1as interacts with these miRNAs in the cytoplasm. We show that Cdr1as is highly expressed (hundreds of copies within neurons) in somas and neurites, but not in glial cells.

ON OUR WEBSITE

Read the full article at http://dx.doi.org/10.1126/science.aam8526

The expression of many immediate early genes (IEGs), which are markers of neuronal activity, was consistently up-regulated in KO animals. For example, *c-Fos* and a few other miR-7 targets were up-regulated, suggesting that IEG up-regulation can in part be explained by miR-7 down-regulation and that Cdr1as modulates neuronal activity. *Cdr1as* KO mice showed a strong deficit in prepulse inhibition of the startle response, a sensorimotor gating phenotype that is impaired in several human neuropsychiatric disorders. Electrophysiological measurements indicated an increase in spontaneous vesicle release in *Cdr1as* KO neurons, suggesting that Cdr1as plays a role in regulating synaptic transmission.

CONCLUSION: Mechanistically, our data indicate that Cdr1as regulates miR-7 stability or transport in neurons, whereas miR-671 regulates Cdr1as levels. Functionally, our data suggest that Cdr1as and its direct interactions with miRNAs are important for sensorimotor gating and synaptic transmission. More generally, because the brain is an organ with exceptionally high and diverse expression of circRNAs, our data suggest the existence of a previously unknown layer of biological functions carried out by circRNAs. ■

The list of author affiliations is available in the full article online.
*These authors contributed equally to this work.
†Corresponding author. Email: rajewsky@mdc-berlin.de
Cite this article as M. Piwecka *et al.*, *Science* **357**, eaam8526 (2017). DOI: 10.1126/science.aam8526

RESEARCH ARTICLE

NEUROBIOLOGY

Loss of a mammalian circular RNA locus causes miRNA deregulation and affects brain function

Monika Piwecka,[1]* Petar Glažar,[1]* Luis R. Hernandez-Miranda,[2]* Sebastian Memczak,[1,3] Susanne A. Wolf,[4] Agnieszka Rybak-Wolf,[1] Andrei Filipchyk,[1] Filippos Klironomos,[1] Cledi Alicia Cerda Jara,[1] Pascal Fenske,[5] Thorsten Trimbuch,[5] Vera Zywitza,[1] Mireya Plass,[1] Luisa Schreyer,[1] Salah Ayoub,[1] Christine Kocks,[1] Ralf Kühn,[6,7] Christian Rosenmund,[5] Carmen Birchmeier,[2] Nikolaus Rajewsky[1]†

Hundreds of circular RNAs (circRNAs) are highly abundant in the mammalian brain, often with conserved expression. Here we show that the circRNA Cdr1as is massively bound by the microRNAs (miRNAs) miR-7 and miR-671 in human and mouse brains. When the *Cdr1as* locus was removed from the mouse genome, knockout animals displayed impaired sensorimotor gating—a deficit in the ability to filter out unnecessary information—which is associated with neuropsychiatric disorders. Electrophysiological recordings revealed dysfunctional synaptic transmission. Expression of miR-7 and miR-671 was specifically and posttranscriptionally misregulated in all brain regions analyzed. Expression of immediate early genes such as *Fos*, a direct miR-7 target, was enhanced in *Cdr1as*-deficient brains, providing a possible molecular link to the behavioral phenotype. Our data indicate an in vivo loss-of-function circRNA phenotype and suggest that interactions between Cdr1as and miRNAs are important for normal brain function.

In recent years, it has been shown that animals express large numbers of single-stranded RNA molecules that are covalently closed at the 5′ and 3′ ends, known as circular RNAs (circRNAs) (*1*–*3*). All mammalian circRNAs studied to date are consequences of "backsplicing," in which the spliceosome joins the 3′ end of an exon with an upstream 5′ end of the same or different exons from the same transcript (*4*–*6*). Backsplicing is context-dependent (*4*, *7*), and circRNAs are often tissue- and developmental stage–specifically expressed (*3*). In mammals, a few hundred circRNAs are highly expressed in major brain areas, with frequently conserved expression between humans and mice (*7*). In neurons, circRNAs are expressed in the soma and neurites and have the overall highest concentration at synaptosomes (*7*, *8*). Probably because of the absence of 5′ and 3′ ends, circRNAs have half-lives ranging from hours to days or longer and are therefore generally much more stable than linear coding or noncoding messages (*3*). Thus, circRNAs may carry out biological functions that differ from those of other classes of RNAs; however, their normal functions are largely unknown.

Cdr1as is a circularized long noncoding RNA (lncRNA) that is highly abundant in the mammalian brain and expressed at low levels or absent in other tissues and organs. It is highly conserved across mammals and not detectable as a linear transcript (*3*, *9*, *10*). Human CDR1as, which is mainly located in the cytoplasm, has more than 70 binding sites for the microRNA (miRNA) miR-7 (*3*, *9*), which is involved in regulation of a number of genes in the brain (*11*–*13*). Binding of miR-7 to CDR1as has been shown in cell lines, and, consequently, CDR1as has been proposed to function as a sponge for miR-7 by reducing the number of freely available miR-7 molecules (*3*, *9*). The miR-7 binding sites are only partially complementary to miR-7, ensuring that Cdr1as is not sliced by AGO2 bound to miR-7:Cdr1as complexes. Cdr1as also has a binding site for miR-671 (*10*). This binding site, in contrast to those for miR-7, has almost full complementarity to miR-671 and therefore may be used by miR-671 to mediate slicing of Cdr1as (*10*), potentially to release its miR-7 cargo. However, the normal in vivo function of Cdr1as has yet to be determined.

Cdr1as binding by miR-7 and miR-671 in the mammalian brain

To identify miRNAs that bind Cdr1as in the mammalian brain, we utilized the recent finding that after RNA:protein purification of the miRNA effector AGO via cross-linking and immunoprecipitation (CLIP) assays, the 3′ end of miRNAs can be ligated to the 5′ end of their RNA target sites. After sequencing, these so-called "chimeras" allow unambiguous in vivo detection of miRNA target sites, as well as, simultaneously, the identification of the individual miRNAs bound to them (*14*). Using our computational pipeline for chimera detection (*14*), we identified and mapped tens of thousands of chimeras in recently published AGO CLIP data from mouse and human postmortem brains (*15*, *16*). When ranking these transcripts by the number of miR-7 chimeras mapping to an individual transcript, the top-scoring target of all transcripts in both human and mouse brains was Cdr1as (Fig. 1A and table S1). Only one other miRNA was highly bound to Cdr1as, miR-671 (Fig. 1A). However, in contrast to miR-7, for which we detected many distinct binding sites on Cdr1as, we detected only one main binding site for miR-671 (Fig. 1A and table S1). The architectures of the miR-7 and miR-671 binding sites are also very different. Whereas miR-7 binding sites feature complementarity only to the 5′ end ("seed" region, which is essential for binding of miRNA to mRNA) of miR-7, the miR-671 binding site is almost perfectly complementary to the entire mature miR-671 sequence (fig. S1). Therefore, miR-671 can mediate slicing of Cdr1as, whereas miR-7 cannot. These binding site architectures are perfectly conserved in mammalian evolution (fig. S1), indicating that they are linked to the function of Cdr1as.

In our chimera analysis, the lncRNA Cyrano (1700020I14Rik) was identified as the second-highest-ranked RNA interacting with miR-7 in the mouse brain (table S1). Cyrano harbors a single, nearly perfectly complementary and highly conserved binding site for miR-7 (*17*). These observations imply that, second to Cdr1as, Cyrano may play an important role in the regulation of miR-7 in the central nervous system.

Neural expression pattern of Cdr1as

To determine Cdr1as expression patterns in the mouse brain, we performed RNA fluorescence in situ hybridization (FISH) in adult brain sections (Fig. 1B and figs. S2 to S4). Costaining with neural markers revealed that Cdr1as was highly expressed in neurons but not expressed in glial cells such as oligodendrocytes and astrocytes (Fig. 1B and fig. S3D). Further, an overlap with excitatory and inhibitory neuronal markers showed that Cdr1as was predominantly expressed in excitatory neurons (Fig. 1, B and C, and figs. S2 to S4). In the cortex, hippocampus, midbrain, and hindbrain, the majority of neurons expressing Cdr1as were VGLUT1- and VGLUT2-positive (figs. S2, B to E; S3, A to C; and S4,

[1]Laboratory for Systems Biology of Gene Regulatory Elements, Berlin Institute for Medical Systems Biology, Max Delbrück Center for Molecular Medicine, Robert-Rössle-Straße 10, Berlin-Buch, Germany. [2]Laboratory for Developmental Biology and Signal Transduction, Max Delbrück Center for Molecular Medicine, Robert-Rössle-Straße 10, Berlin-Buch, Germany. [3]Experimental and Clinical Research Center, Charité Medical Faculty and Max Delbrück Center for Molecular Medicine, Robert-Rössle-Straße 10, Berlin-Buch, Germany. [4]Laboratory for Cellular Neurosciences, Max Delbrück Center for Molecular Medicine, Robert-Rössle-Straße 10, Berlin-Buch, Germany. [5]Department of Neurophysiology, NeuroCure Cluster of Excellence, Charité-Universitätsmedizin, Berlin, Germany. [6]Transgenic Core Facility, Max Delbrück Center for Molecular Medicine, Robert-Rössle-Straße 10, Berlin-Buch, Germany. [7]Berlin Institute of Health, Kapelle-Ufer 2, Berlin, Germany. *These authors contributed equally to this work. †Corresponding author. Email: rajewsky@mdc-berlin.de

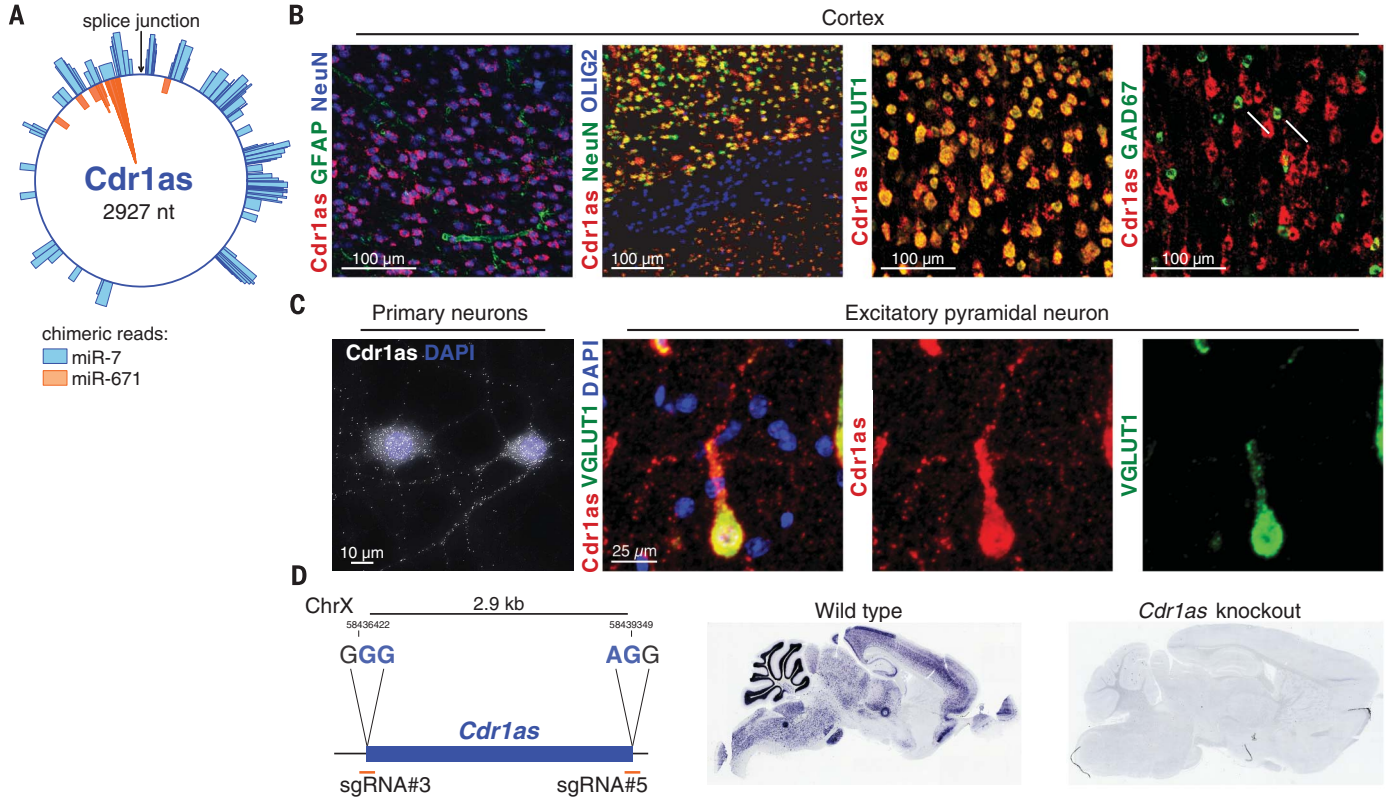

Fig. 1. The circRNA Cdr1as is bound by miR-7 and miR-671 and highly expressed in excitatory neurons. (**A**) Cdr1as is densely bound by AGO:miRNA complexes containing miR-7 and miR-671. Bars on the circle represent circRNA:miRNA chimeric reads from AGO2 HITS-CLIP data from mouse brains. (**B**) Cdr1as is predominantly expressed in excitatory as opposed to inhibitory neurons and is not detected in glial cells. Markers: GFAP, astrocytes; NeuN, neurons, OLIG2, oligodendrocytes; VGLUT1, excitatory neurons; GAD67, inhibitory neurons. Arrows mark Cdr1as expression overlap with inhibitory neurons. Cdr1as, VGLUT1, and GAD67 mRNAs were detected by in situ hybridization (ISH) and GFAP, NeuN, and OLIG2 by immunostainings. (**C**) Cdr1as is broadly distributed in neuronal somas and neurites. Leftmost panel, single-molecule fluorescent in situ hybridization (FISH) for Cdr1as in cultured primary cortical neurons [in vitro day 14; DAPI (4′,6-diamidino-2-phenylindole) nuclear staining]. Right three panels, single excitatory pyramidal neuron at lamina II. (**D**) Using CRISPR-Cas9, the *Cdr1as* locus was deleted. The sequences given (left) denote protospacer adjacent motifs. kb, kilobases. RNA ISH (right) confirmed successful genetic ablation of *Cdr1as*.

B and D). In the cerebellum, Cdr1as expression was observed exclusively in the granular layer with a high content of excitatory neurons and did not overlap with GABAergic neurons present in the molecular layer and Purkinje cells (fig. S4D; GABA, γ-aminobutyric acid). Single-molecule RNA FISH in primary cortical neurons revealed Cdr1as expression in both soma and neurites (Fig. 1C, left), indicating a possible functional role of Cdr1as in different subcellular localizations.

Cdr1as loss-of-function mutant mice

Because Cdr1as is so efficiently circularized in human and mouse cells that it cannot be detected as a linear transcript (*3*, *9*, *10*), the most straightforward strategy to create a loss-of-function (LoF) mouse model for this circRNA is to remove the *Cdr1as* locus by using CRISPR-Cas9. However, this strategy could also affect transcription on the other strand and therefore complicate the interpretation. To evaluate expression from the other strand, we created and sequenced 24 stranded RNA libraries (i.e., retaining the strand-of-origin information in the RNA sequencing library) from four mouse brain regions, performed in situ hybridization (ISH) with a probe complementary to the putative sense transcript (Cdr1 mRNA), and analyzed published RNA sequencing, cap analysis of gene expression, and chromatin modification data (fig. S5). We failed to detect any evidence for transcription of the strand opposite to *Cdr1as* in mouse brains, specific mouse brain regions, or any other mouse or human tissue analyzed. We therefore removed the *Cdr1as* locus (Fig. 1D) from the mouse genome, as shown by genotyping (fig. S6, A and B), ISH (Fig. 1D and fig. S6C), Northern blot analysis (fig. S6D), and quantitative reverse transcription polymerase chain reaction (qRT-PCR) assays (fig. S7A). *Cdr1as* knockout (KO) mice were viable and fertile and displayed no gross abnormality in adult brain anatomy (fig. S6E).

Because *Cdr1as* is X-linked, before analysis of KO animals, we investigated Cdr1as expression in wild-type (WT) male and female and heterozygous ($Cdr1as^{+/-}$) female brains. qRT-PCR assays showed that Cdr1as expression in male and female WT mice was about equal, whereas in heterozygous female mice, Cdr1as levels were reduced by ~50% relative to the WT levels (fig. S7B). Because there were no differences in Cdr1as expression levels between WT males and females, we used hemizygous ($Cdr1as^{-/Y}$) male mice for further molecular analysis.

miR-7 and miR-671 are posttranscriptionally deregulated in *Cdr1as* KO brains

We sequenced miRNAs in four major brain regions (cerebellum, cortex, hippocampus, and olfactory bulb) where Cdr1as is highly expressed (*7*). Northern blot analysis was also used to detect miR-7 in assayed tissues (fig. S8). When comparing expression levels from our sequencing data in WT and KO animals, miR-7 was consistently and markedly down-regulated (Fig. 2 and statistics in table S2). More precisely, both miR-7a-5p and miR-7b-5p, which have the same seed but slightly different mature sequences and are produced from three different miR-7 loci in the genome, were down-regulated to comparable levels in all cases. This down-regulation was highly specific. From hundreds of identified miRNAs, only eight miRNAs other than miR-7a-5p and miR-7b-5p were significantly down-regulated,

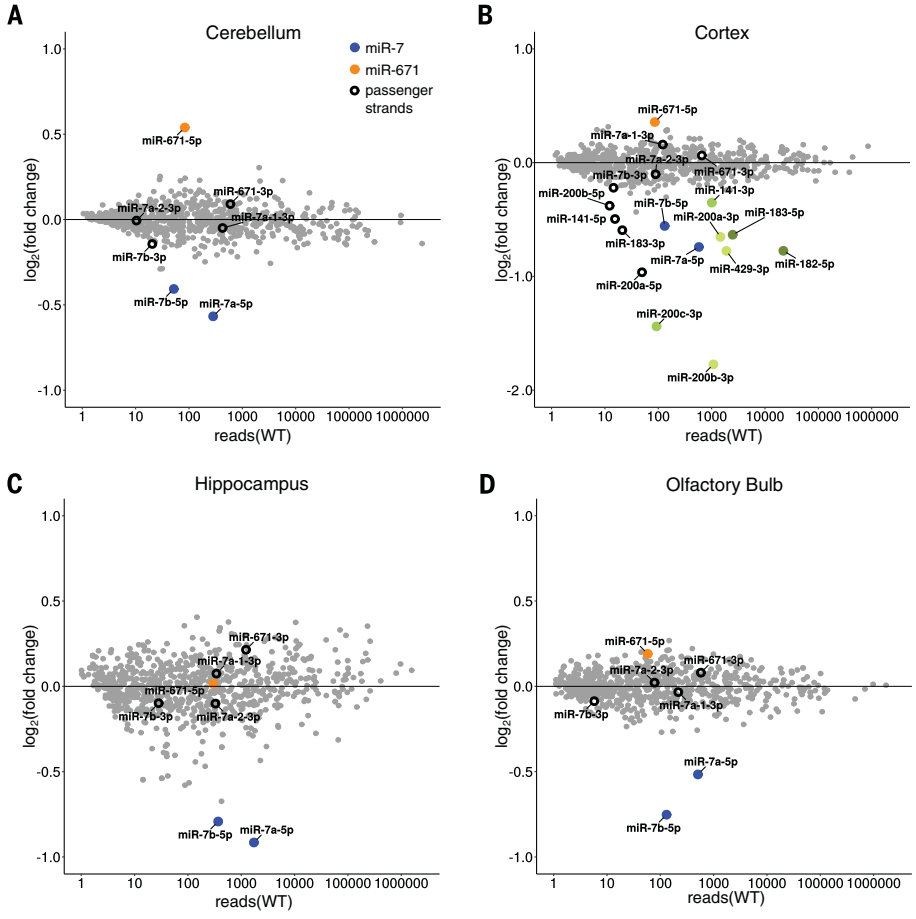

Fig. 2. miRNA expression changes in *Cdr1as* knockout (KO) brain regions. Small RNAs were sequenced from mouse (**A**) cerebellum, (**B**) cortex, (**C**) hippocampus, and (**D**) olfactory bulb, each in biological replicates of $n = 3$, except *Cdr1as* KO hippocampus ($n = 2$). Shades of green indicate miRNAs of the same family. Gray, miRNAs with no significant expression change. WT, wild type.

and this occurred only in the cortex (Fig. 2B). All of these miRNAs belong to two families and are derived from three primary transcripts (miR-200c/141, miR-200a/200b/429, and miR-182/183/96). We confirmed miR-7 down-regulation in all four brain regions by Northern blot (Fig. 3A and fig. S9), ISH (Fig. 3, B and C), and qRT-PCR assays (fig. S7C). In addition, miR-7 down-regulation was posttranscriptional. This finding is supported by the sequencing data showing that none of the three miR-7 passenger strands (miR-7a-1-3p, miR-7a-2-3p, and miR-7b-3p), which are respectively processed from the three distinct miR-7 precursors, were significantly deregulated (Fig. 2). This observation was validated by Northern blot (fig. S9A) and an independent qRT-PCR assay for pre–miR-7a-1 (fig. S7D). Pre–miR-7a-2 and pre–miR-7b were below reliable detection levels in qRT-PCR analysis. The down-regulated expression of miRNAs from miR-200 and miR-183 families in the cortex was probably the result of a transcriptional effect, given that the corresponding passenger strands were also down-regulated (Fig. 2B). Unlike miR-7 expression, miR-671-5p expression in KO animals was up-regulated in the cerebellum, cortex, and olfactory bulb (Fig. 2, A, B, and D). But as with miR-7, this deregulation in KO mice was highly specific: Aside from miR-671, no other miRNA was consistently up-regulated. Also like miR-7, miR-671-5p was deregulated posttranscriptionally, as evidenced by unperturbed passenger strand expression (Fig. 2, A, B, and D). Northern blot analysis failed to detect mature miR-671-5p in either KO or WT RNA extracts, although miR-671-3p was detectable and remained unaltered (fig. S9A). Two reasons may explain why miR-671-5p and its precursor are difficult to detect: (i) Mature miR-671 is lowly expressed and unstable, as shown in metabolic labeling experiments (*18*), and (ii) the precursor is processed from the coding sequence of the well-expressed *Chpf2* transcript.

We analyzed Cdr1as, miR-7, and miR-671 levels in nonbrain tissues including lung, skeletal muscle, spleen, heart, and spinal cord (fig. S7, A, C, and E). In the spleen, where Cdr1as was undetectable but miR-7a was well-expressed, and in other tissues exhibiting very low expression of Cdr1as, miR-7a levels were not changed by *Cdr1as* removal. The only nonbrain tissue with substantially changed miR-7 expression was spinal cord. This was also the only nonbrain tissue for which we detected reasonable expression of Cdr1as, consistent with the expression of Cdr1as in neurons and neuronal projections.

Taken together, these data show that loss of Cdr1as does not affect miR-7 and miR-671 in tissues outside the brain that normally exhibit very low levels of Cdr1as RNA, whereas Cdr1as loss drives down-regulation of miR-7 in neural tissues of KO animals. We conclude that there is a highly specific, posttranscriptional deregulation of miR-7 and miR-671 in the brains of *Cdr1as* KO animals. These are the two miRNAs that we identified by in vivo chimera analysis as directly interacting with Cdr1as.

Up-regulation of immediate early genes, including miR-7 targets, in *Cdr1as* KO brains

To assess the functional consequences of Cdr1as removal, we measured changes in mRNA expression by sequencing mRNAs in the same brain regions in which we observed miR-7 and miR-671 deregulation: the cerebellum, cortex, hippocampus, and olfactory bulb (Fig. 4, A to D, and table S3). Conserved miR-7 targets (*19*) were significantly up-regulated in the cortex, cerebellum, and olfactory bulb (Mann-Whitney *U* test; $P < 10^{-4}$, 10^{-3}, and 10^{-7}, respectively) (fig. S10), including several validated miR-7 targets, such as *Fos* (which has three conserved binding sites in its 3′ untranslated region) (*20*), *Nr4a3* (*21*), *Irs2* (*22*), and *Klf4* (*23*) (Fig. 4, A to D; fig. S11; and statistics in tables S3 and S4). The lncRNA Cyrano—which interacts with miR-7 in the brain, as supported by Cyrano:miR-7 chimeras (table S1)—was highly expressed and stable in all analyzed brain regions of *Cdr1as* KO animals. Furthermore, among the genes that were up-regulated in each of the four brain regions, we found an obvious and highly significant overrepresentation (hypergeometric test; $P < 10^{-33}$) of immediate early genes (IEGs), such as *Fos*, *Arc*, *Egr1*, *Egr2*, *Nr4a3*, and others, which are part of the first wave of response to different stimuli and markers of neuronal activity (Fig. 4, A to D; fig. S11; and tables S3 and S4). We validated the sequencing data by qRT-PCR assays (fig. S12) and Nanostring (fig. S13A and table S5), using the cortex and hippocampus from the same and independent animals. We confirmed an increased expression of IEGs at the protein level for all tested candidates. Elevated levels of c-Fos, EGR1, and ARC were detected by Western blots (Fig. 4E) and by further immunohistochemical validation of c-Fos and EGR1 proteins in brain sections (Fig. 4F and figs. S14 to S16). Quantification of c-Fos immunostaining performed in four cortical regions showed a consistent increase in both the number of neurons expressing c-Fos and the c-Fos signal intensity in KO brains (fig. S15). These data are important for two reasons. First, miR-7 is a known repressor of the cell cycle and IEGs such as *Fos*, suggesting a direct link between Cdr1as removal and up-regulation of IEGs. Second, up-regulation of IEGs is strongly linked to increased activity of neurons (*24*–*26*). Therefore, we conclude that

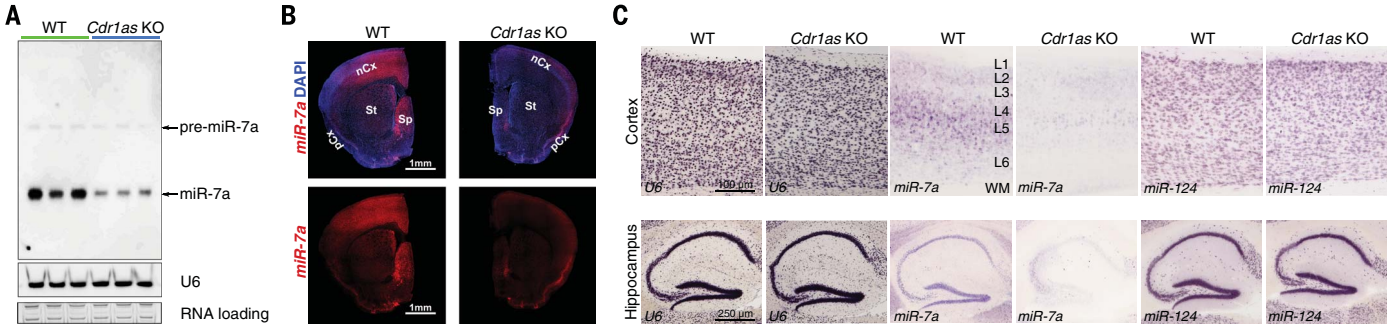

Fig. 3. miR-7a is down-regulated in *Cdr1as* KO brains. miRNA-7a expression in *Cdr1as* KO and WT mouse brains detected using (**A**) Northern blotting, (**B**) FISH, and (**C**) chromogenic ISH. nCx, neocortex; St, striatum; Sp, septum; pCx, piriform cortex; L1 to L6, cortical layers; WM, white matter; U6 and miR-124, control RNAs.

the reduction of miR-7 followed by enhanced expression of IEGs implies higher neuronal activity in *Cdr1as* KO brains, and we hypothesized that this effect has further functional consequences at the phenotypic level.

Consistent with the expression pattern of Cdr1as, the expression levels of IEGs in non-brain tissues of KO animals remained unaltered (fig. S13, B to E), suggesting that the observed effect is brain-specific. We also observed that, in addition to IEGs, there were several differentially expressed circadian clock genes in *Cdr1as* KO brains. *Per1* and *Sik1* were consistently up-regulated, and *Dbp* was consistently down-regulated (Fig. 4, A to D). This expression pattern in the forebrain has previously been associated with sleep deprivation and extended wakefulness in mice (*27*, *28*).

Dysfunction of excitatory synaptic transmission in *Cdr1as* KO mice

Given that Cdr1as is predominantly expressed in excitatory neurons (Fig. 1, B and C, and figs. S2 to S4), we wanted to elucidate the physiological consequences of removing Cdr1as at the synaptic level. Therefore, we used single hippocampal neurons and studied excitatory postsynaptic currents (EPSCs). We found that spontaneous vesicle release was strongly up-regulated in the KO neurons, with more than a doubling of miniature EPSC frequency (Fig. 5A) but not amplitude (fig. S17A). By analyzing calcium-evoked synaptic responses, we found that the EPSC amplitude of *Cdr1as* KO neurons was not significantly different from that of WT neurons (Fig. 5B, left). The observed effect of higher spontaneous release was not dependent on synapse formation or vesicle priming activity, because the size of the readily releasable vesicle pool was not significantly altered (fig. S17B). Although the computed vesicular release probability also was not significantly altered (fig. S17B), responses to two consecutive stimuli (Fig. 5B, right) and to a train of action potentials at 10 Hz were differentially modulated in the KO and WT neurons (fig. S17C). This suggests altered vesicle replenishment dynamics during ongoing synaptic release activity and stronger depression in the synaptic response in the KO neurons.

These electrophysiological recordings indicate that Cdr1as deficiency leads to a dysfunction of excitatory synaptic transmission. Possible mechanisms that could explain this change include changes in expression of synaptic proteins (*29*), malformation of synaptic specialization, or alteration in synaptic calcium homeostasis (*30*).

Neuropsychiatric-like alteration in the behavior of *Cdr1as* KO mice

To further evaluate the biological implications of miRNA and IEG deregulation in *Cdr1as* KO brains, we performed behavioral assays with WT and *Cdr1as* KO animals (Fig. 5C, fig. S18, and table S6). *Cdr1as* KO mice showed normal social behavior, unaffected anxiety levels, unperturbed locomotor activity in an open field test, and no significant deficits in recognition memory or exploratory behavior (fig. S18, B to H). However, a test of prepulse inhibition (PPI) of the startle response revealed a significant and strong difference (30 to 50%) between WT and *Cdr1as* KO mice (both males and females) at all three prepulse intensities (Fig. 5C). PPI is used to detect defects in the normal suppression of the startle response that occurs when a startle-eliciting stimulus is preceded by a low-intensity prestimulus (the prepulse). It is a measure of sensorimotor gating that is impaired in schizophrenia and some other psychiatric diseases in humans and used in animal models of endophenotypes related to neuropsychiatric disorders (*31*–*34*). The impairment was evident and specific for the inhibition of the startle response. The baseline response to the pulse only (120 dB) was similar across genotypes and groups (fig. S18A). Therefore, the PPI deficiency is not due to differences in the response to an acoustic stimulus or due to hearing impairments.

Thus, our data show that *Cdr1as* KO animals exhibit a behavioral phenotype associated with neuropsychiatric disorders—namely, a strong sensorimotor gating deficit. Our findings support the general observation that up-regulation of IEGs such as *Fos*, *Egr1*, and *Egr4* is linked to reduced PPI (*35*).

Discussion

In this study, we used CRISPR-Cas9 to remove the locus encoding Cdr1as, a circRNA that is highly expressed in neurons and predominantly localized to the cytoplasm. In all tested in vivo mammalian tissues and cell lines, Cdr1as was detected only as a circRNA (*3*, *9*, *10*). We failed, by different assays, to detect any transcription on the strand antisense to *Cdr1as*, making it unlikely that removal of the *Cdr1as* locus has consequences beyond removing the circRNA. We cannot rule out CRISPR-Cas9 off-target effects or other unspecific consequences for the locus, but these (if existent) are unlikely to have contributed to the molecular and behavioral phenotype that we observed in the KO animals. This is because (i) we show that precisely the two miRNAs (miR-7 and miR-671) that we found to specifically interact with Cdr1as in the brain are deregulated in the KO animals; (ii) IEGs, including direct targets of miR-7, are up-regulated in the mutant brains but not in other tissues where Cdr1as is very lowly or not expressed; (iii) IEGs are already known to be linked to the observed neuropsychiatric symptom, impaired prepulse inhibition (PPI) (*35*); and (iv) Cdr1as is exclusively expressed in neurons but not glial cells, suggesting that Cdr1as interactions with miRNAs are functional in neurons, in line with the observed deficit in PPI and dysfunction in synaptic transmission.

How can we explain the specific and opposite deregulation of miR-7 and miR-671 upon loss of Cdr1as? The reason may lie in the very different and highly conserved architectures of the binding sites of miR-7 and miR-671 on Cdr1as. None of the >70 miR-7 binding sites has extensive complementarity beyond the seed region, indicating that miR-7 stably binds but cannot slice Cdr1as. In contrast, miR-671 has one main binding site with almost perfect complementarity, which should lead to slicing of Cdr1as (*10*) and may cause tailing and trimming (removal) of miR-671 (*36*, *37*). Thus, upon depletion of Cdr1as, we would expect up-regulation of miR-671 and down-regulation of miR-7, which is no longer stabilized by Cdr1as.

Is miR-7 turnover upon *Cdr1as* KO a passive decay process, or is it regulated? We speculate that miR-7 decay is promoted and regulated by the lncRNA Cyrano (*17*). This is because (i) we found Cyrano to be the second-highest miR-7

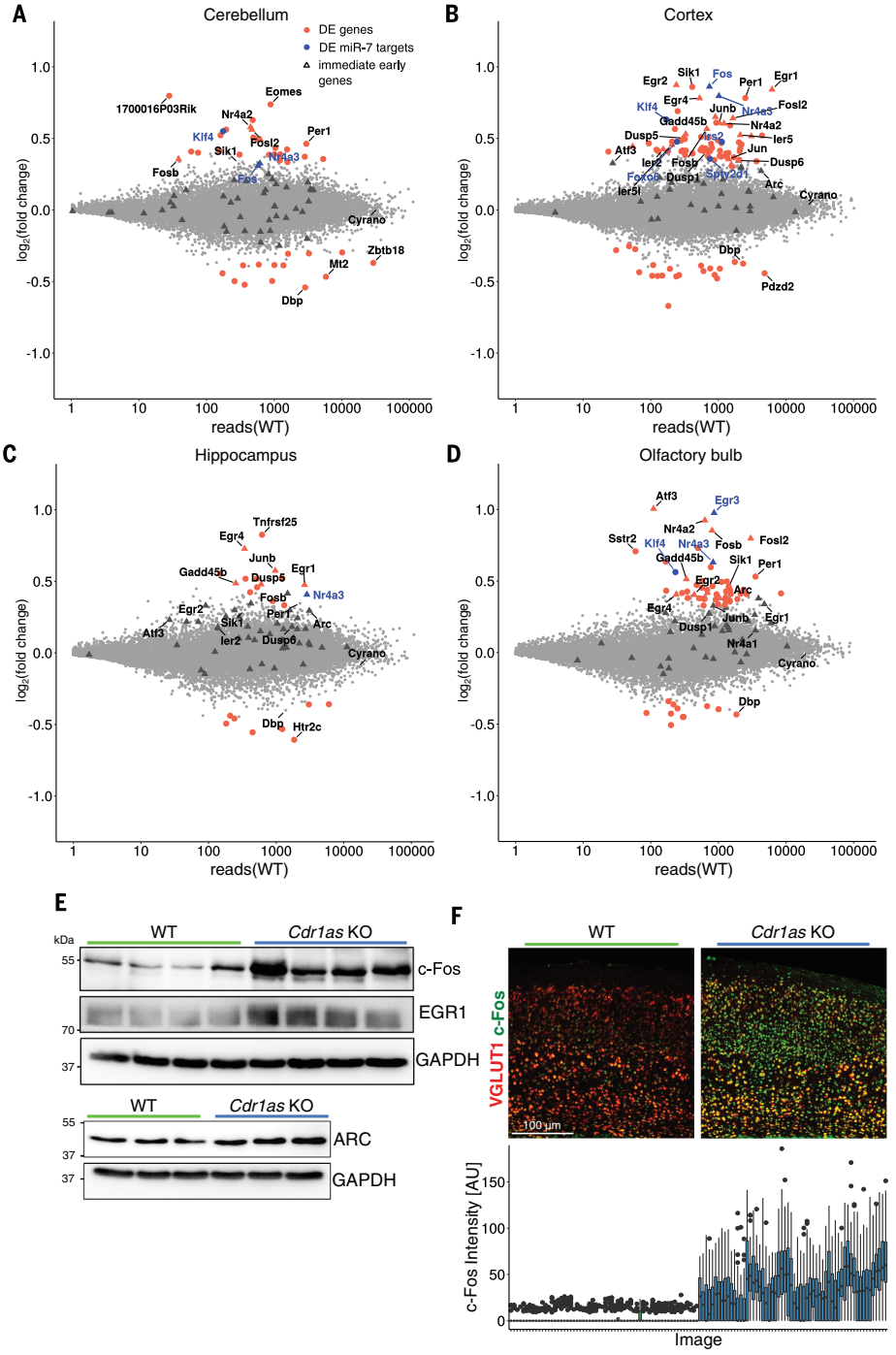

Fig. 4. Gene expression changes in *Cdr1as* KO brains. Polyadenylated RNAs were sequenced from mouse (**A**) cerebellum, (**B**) cortex, (**C**) hippocampus, and (**D**) olfactory bulb, each in biological replicates of $n = 3$. DE, significantly differentially expressed; gray, no significant expression change. (**E**) Western Blot analysis of differentially expressed immediate early genes in cortical lysates; GAPDH serves as a loading control. (**F**) Top, c-Fos immunohistochemistry combined with ISH for VGLUT1 mRNA in the somatosensory cortex. Bottom, c-Fos signal intensity quantification across images ($n = 60$ per genotype). Boxes are defined by the first and third quartiles; horizontal bars, medians; whiskers span 1.5 times the interquartile range; gray circles, outliers; AU, arbitrary units.

interactor in chimeric data (table S1); (ii) Cyrano was highly expressed in all tissues in which we detected Cdr1as expression (Fig. 4, A to D); and (iii) the miR-7 binding site on Cyrano is unusual in that it has an extremely well conserved architecture that, similar to the miR-671 binding site on Cdr1as, could promote miR-7 removal by tailing and trimming (*17*, *36*, *37*).

When comparing mRNA expression between WT and KO animals, we found an enrichment of up-regulated IEGs, some of which, such as *Fos* and *Nr4a3*, are known miR-7 targets. Up-regulation of predicted miR-7 targets was statistically significant, consistent with the observed reduction of miR-7. The known miR-7 targets *Klf4*, *Nr4a3*, and *Irs2*, which were increased in KO postnatal cortex, were also up-regulated in a miR-7 knockdown study performed in the embryonic cortex (*13*). However, miR-7 targets did not explain the majority of up-regulation, indicating that we observed a mixture of direct and indirect effects. We also observed different overall responses of miR-7 targets in the mouse brain upon constitutive *Cdr1as* knockout, compared with results from knockdown experiments in human embryonic kidney–293 cells, in which targets of miR-7 were repressed (*3*). We argue that there are different scenarios for what may happen to miR-7 bound to Cdr1as if Cdr1as is removed from a cellular system conditionally versus constitutively. A scenario in which miR-7:RISC complexes could be released and subsequently down-regulate miR-7 targets may be more plausible when Cdr1as is conditionally knocked down. In a situation in which Cdr1as is constitutively knocked out, miR-7 molecules not stabilized by the circRNA may be more likely to be turned over. Thus, miR-7 targets can be up-regulated. Additionally, the widespread distribution of Cdr1as in neuronal processes argues for a functional role of Cdr1as in the transport of miR-7:AGO complexes and provides another layer of complexity to the regulation of miR-7 targets, which could be differential in various subcellular localizations. miR-671 therefore may provide an "unlocking" mechanism that serves to slice Cdr1as under specific conditions within the cell to release the cargo (sponged miR-7:AGO complexes). It will be interesting to test these hypotheses, but the lack of suitable in vitro systems, the technical difficulties in performing efficient and conditional overexpression or knockdown of Cdr1as, and the complex phenotypes observed will likely require the generation of many transgenic cell and mouse lines. In any case, activation of IEGs has been linked to increased neuronal activity, which can be induced by both cell-extrinsic and cell-intrinsic signals (*38*, *39*) and has further functional consequences—for example, in synaptic plasticity and memory formation (*40*).

In behavioral tests, *Cdr1as* KO animals displayed significant and strong PPI impairment, a neuropsychiatric phenotype. A deficit in PPI manifests as the inability to effectively attenuate the intrinsic startle response to redundant stimuli. PPI deficit correlates clinically with symptoms such as thought disorder and distractibility in schizophrenia; therefore, PPI has emerged as a promising endophenotype in human and rodent models of the disease (*31*, *33*, *41*). Reduced PPI is also a hallmark of other neuropsychiatric disorders, including obsessive-compulsive disorder, bipolar disorder, Tourette syndrome, post-traumatic stress disorder, Huntington's disease, and Asperger syndrome (*34*, *42*). PPI is a complex phenotype that involves diverse neural systems

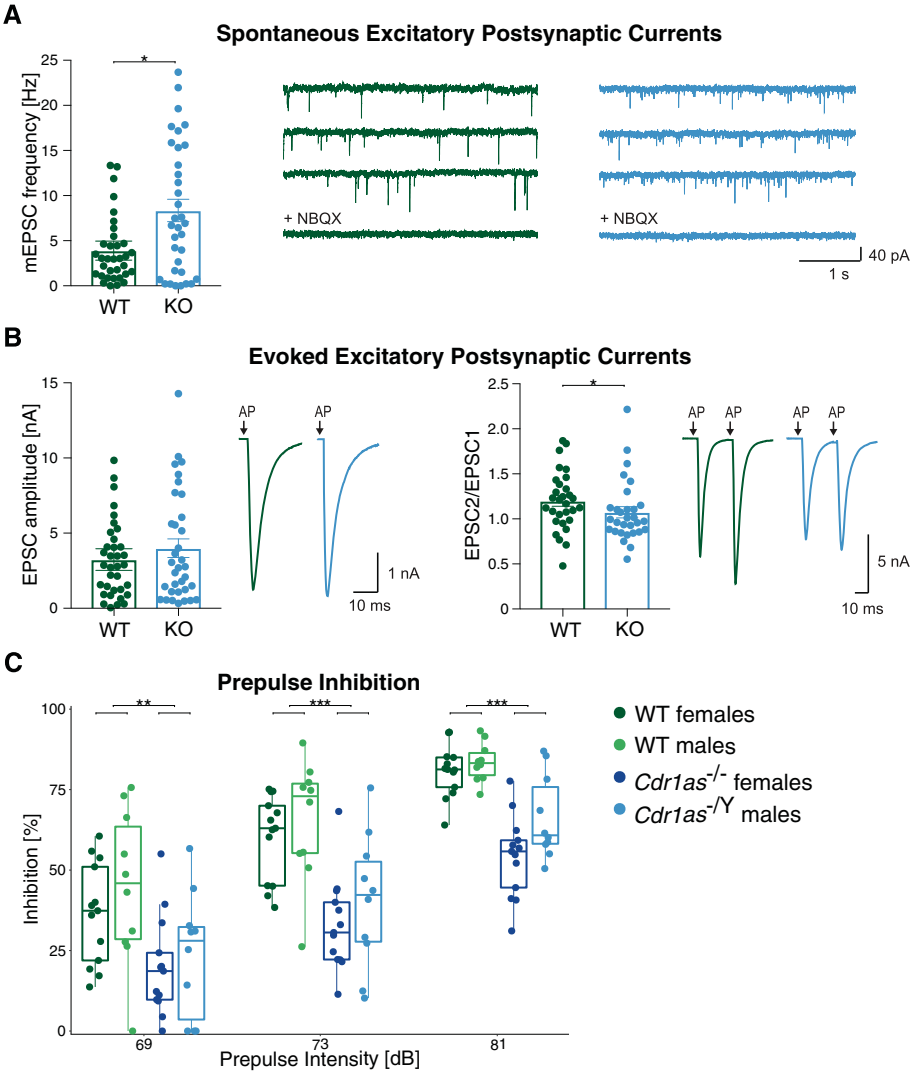

Fig. 5. Loss of *Cdr1as* locus contributes to dysfunctional synaptic neurotransmission and abnormal brain function associated with neuropsychiatric disorders. (**A** and **B**) *Cdr1as* KO neurons showed increased spontaneous vesicle release and normal calcium-evoked excitatory postsynaptic currents (EPSCs). The left panel of (A) shows miniature EPSC (mEPSC) frequencies of WT (n = 34) and *Cdr1as* KO (n = 34) autaptic neurons. Right panel of (A), representative traces from WT (green) and *Cdr1as* KO (blue) in standard extracellular solution and in AMPA receptor–blocking NBQX (2,3-dihydroxy-6-nitro-7-sulfamoylbenzo[*f*]quinoxaline) solution. The left panel of (B) shows EPSC amplitudes of WT (n = 35) and *Cdr1as* KO (n = 34) neurons. Right panel of (B), 25-ms interstimulus interval paired-pulse ratio for WT (n = 30) and *Cdr1as* KO (n = 30) neurons. Representative traces of evoked EPSCs are shown. Time of action potentials (AP) are indicated by arrows, and currents associated with AP induction were blanked to enhance visibility of the synaptic current. Mann-Whitney U test; $^*P < 0.05$. All data are represented as means ± SEM. (**C**) *Cdr1as* KO mice showed deficits in prepulse inhibition (PPI) of the startle reflex. PPI was measured as the percentage of the basal startle response. WT females, n = 13; *Cdr1as* KO females, n = 13; WT males, n = 10; *Cdr1as* KO males, n = 10. Boxes are defined by the first and third quartiles; medians are indicated as horizontal bars; whiskers span 1.5 times the interquartile range. Three-way analysis of variance with Bonferroni-corrected Welch t test; $^{**}P < 0.01$, $^{***}P < 0.001$. Because there was no significant effect of gender, the male and female mice were pooled in post hoc tests.

encompassing the brainstem, pedunculopontine, hippocampus, amygdala, and prefrontal cortical regions, as well as different neurochemical substrates including dopamine, glutamate, and GABA (*43*). According to our analysis, Cdr1as is expressed in most excitatory neurons. After removing the *Cdr1as* locus, we observed a disrupted excitatory neurotransmission reflected as an increased spontaneous vesicle release and stronger depression in synaptic response upon enhanced neuronal activity in KO neurons. It is interesting that miR-7 has been described as a negative regulator of vesicle release in pancreatic β cells (*44*). Our findings suggest that loss of Cdr1as destabilizes mature miR-7 in neurons, which results in de-repression of IEGs and leads to altered neuronal activity, which may cause the sensorimotor deficits and the neuropsychiatric phenotype. In addition to miR-7, miR-200 was also strongly deregulated in the cortex and may contribute to the observed phenotype. Given the broad expression of Cdr1as in the brain and the diversity of the neural systems recruited in PPI, these hypotheses need thorough testing.

We focused on behavior and synaptic functions. However, we noticed that genes specifically for circadian clock regulation were consistently deregulated in KO brains. Moreover, deregulation of miR-7, miR-671, the miR-200 family, and IEGs is associated with cancer, which will be important to consider in cancer models in the future.

Methods summary

Cdr1as KO animals were generated using CRISPR-Cas9 via microinjection of one-cell embryos with Cas9 mRNA and two single-guide RNAs (sgRNAs) designed to bind upstream of *Cdr1as* splice sites. The *Cdr1as* KO strain was generated and maintained on the pure C57BL/6N background. Molecular and electrophysiological analyses were performed using KO animals and littermate WT control animals. Behavioral studies were performed using *Cdr1as* KO animals and littermate or age-matched WT control animals. The experimental procedures were approved by the Landesamt für Gesundheit und Soziales (Berlin, Germany).

ISH and immunostainings were performed on fresh frozen brain sections, using locked nucleic acid probes, RNAs obtained by in vitro transcription on PCR products, or commercially available antibodies. Whole-cell voltage-clamp recordings were obtained from *Cdr1as* KO and WT hippocampal autaptic neurons at day 14 to 17 in vitro. cDNA libraries for RNA sequencing were generated according to the Illumina TruSeq protocols and sequenced on an Illumina NextSeq 500 system. Differential gene and miRNA expression analyses were performed using the DESeq2 package. RNA:miRNA chimeric reads were analyzed using previously published AGO HITS-CLIP (high-throughput sequencing of RNA isolated by CLIP) data (*15*, *16*) and an in-house pipeline based on (*14*). The details of experimental procedures, reagents, and computational analyses, including supporting references, are given in the materials and methods section of the supplementary materials.

REFERENCES AND NOTES

1. J. Salzman, C. Gawad, P. L. Wang, N. Lacayo, P. O. Brown, Circular RNAs are the predominant transcript isoform from hundreds of human genes in diverse cell types. *PLOS ONE* **7**, e30733 (2012). doi: 10.1371/journal.pone.0030733; pmid: 22319583
2. W. R. Jeck *et al.*, Circular RNAs are abundant, conserved, and associated with ALU repeats. *RNA* **19**, 141–157 (2013). doi: 10.1261/rna.035667.112; pmid: 23249747
3. S. Memczak *et al.*, Circular RNAs are a large class of animal RNAs with regulatory potency. *Nature* **495**, 333–338 (2013). doi: 10.1038/nature11928; pmid: 23446348

4. R. Ashwal-Fluss *et al*., circRNA biogenesis competes with pre-mRNA splicing. *Mol. Cell* **56**, 55–66 (2014). doi: 10.1016/j.molcel.2014.08.019; pmid: 25242144
5. X. O. Zhang *et al*., Complementary sequence-mediated exon circularization. *Cell* **159**, 134–147 (2014). doi: 10.1016/j.cell.2014.09.001; pmid: 25242744
6. S. Starke *et al*., Exon circularization requires canonical splice signals. *Cell Rep.* **10**, 103–111 (2015). doi: 10.1016/j.celrep.2014.12.002; pmid: 25543144
7. A. Rybak-Wolf *et al*., Circular RNAs in the mammalian brain are highly abundant, conserved, and dynamically expressed. *Mol. Cell* **58**, 870–885 (2015). doi: 10.1016/j.molcel.2015.03.027; pmid: 25921068
8. X. You *et al*., Neural circular RNAs are derived from synaptic genes and regulated by development and plasticity. *Nat. Neurosci.* **18**, 603–610 (2015). doi: 10.1038/nn.3975; pmid: 25714049
9. T. B. Hansen *et al*., Natural RNA circles function as efficient microRNA sponges. *Nature* **495**, 384–388 (2013). doi: 10.1038/nature11993; pmid: 23446346
10. T. B. Hansen *et al*., miRNA-dependent gene silencing involving Ago2-mediated cleavage of a circular antisense RNA. *EMBO J.* **30**, 4414–4422 (2011). doi: 10.1038/emboj.2011.359; pmid: 21964070
11. E. Junn *et al*., Repression of α-synuclein expression and toxicity by microRNA-7. *Proc. Natl. Acad. Sci. U.S.A.* **106**, 13052–13057 (2009). doi: 10.1073/pnas.0906277106; pmid: 19628698
12. A. de Chevigny *et al*., miR-7a regulation of Pax6 controls spatial origin of forebrain dopaminergic neurons. *Nat. Neurosci.* **15**, 1120–1126 (2012). doi: 10.1038/nn.3142; pmid: 22729175
13. A. Pollock, S. Bian, C. Zhang, Z. Chen, T. Sun, Growth of the developing cerebral cortex is controlled by microRNA-7 through the p53 pathway. *Cell Rep.* **7**, 1184–1196 (2014). doi: 10.1016/j.celrep.2014.04.003; pmid: 24813889
14. S. Grosswendt *et al*., Unambiguous identification of miRNA: target site interactions by different types of ligation reactions. *Mol. Cell* **54**, 1042–1054 (2014). doi: 10.1016/j.molcel.2014.03.049; pmid: 24857550
15. R. L. Boudreau *et al*., Transcriptome-wide discovery of microRNA binding sites in human brain. *Neuron* **81**, 294–305 (2014). doi: 10.1016/j.neuron.2013.10.062; pmid: 24389009
16. M. J. Moore *et al*., miRNA-target chimeras reveal miRNA 3′-end pairing as a major determinant of Argonaute target specificity. *Nat. Commun.* **6**, 8864 (2015). doi: 10.1038/ncomms9864; pmid: 26602609
17. I. Ulitsky, A. Shkumatava, C. H. Jan, H. Sive, D. P. Bartel, Conserved function of lincRNAs in vertebrate embryonic development despite rapid sequence evolution. *Cell* **147**, 1537–1550 (2011). doi: 10.1016/j.cell.2011.11.055; pmid: 22196729
18. E. E. Duffy *et al*., Tracking distinct RNA populations using efficient and reversible covalent chemistry. *Mol. Cell* **59**, 858–866 (2015). doi: 10.1016/j.molcel.2015.07.023; pmid: 26340425
19. V. Agarwal, G. W. Bell, J. W. Nam, D. P. Bartel, Predicting effective microRNA target sites in mammalian mRNAs. *eLife* **4**, e05005 (2015). doi: 10.7554/eLife.05005; pmid: 26267216
20. X. D. Zhao *et al*., MicroRNA-7/NF-κB signaling regulatory feedback circuit regulates gastric carcinogenesis. *J. Cell Biol.* **210**, 613–627 (2015). doi: 10.1083/jcb.201501073; pmid: 26261179
21. L. Stevanato, J. D. Sinden, The effects of microRNAs on human neural stem cell differentiation in two- and three-dimensional cultures. *Stem Cell Res. Ther.* **5**, 49 (2014). doi: 10.1186/scrt437; pmid: 24725992
22. K. M. Giles, R. A. Brown, M. R. Epis, F. C. Kalinowski, P. J. Leedman, miRNA-7-5p inhibits melanoma cell migration and invasion. *Biochem. Biophys. Res. Commun.* **430**, 706–710 (2013). doi: 10.1016/j.bbrc.2012.11.086; pmid: 23206698
23. H. Okuda *et al*., miR-7 suppresses brain metastasis of breast cancer stem-like cells by modulating KLF4. *Cancer Res.* **73**, 1434–1444 (2013). doi: 10.1158/0008-5472.CAN-12-2037; pmid: 23384942
24. W. C. Abraham *et al*., Correlations between immediate early gene induction and the persistence of long-term potentiation. *Neuroscience* **56**, 717–727 (1993). doi: 10.1016/0306-4522(93)90369-Q; pmid: 8255430
25. J. I. Morgan, D. R. Cohen, J. L. Hempstead, T. Curran, Mapping patterns of c-fos expression in the central nervous system after seizure. *Science* **237**, 192–197 (1987). doi: 10.1126/science.3037702; pmid: 3037702
26. J. F. Guzowski, B. L. McNaughton, C. A. Barnes, P. F. Worley, Environment-specific expression of the immediate-early gene *Arc* in hippocampal neuronal ensembles. *Nat. Neurosci.* **2**, 1120–1124 (1999). doi: 10.1038/16046; pmid: 10570490
27. J. P. Wisor *et al*., A role for cryptochromes in sleep regulation. *BMC Neurosci.* **3**, 20 (2002). doi: 10.1186/1471-2202-3-20; pmid: 12495442
28. P. Franken, R. Thomason, H. C. Heller, B. F. O'Hara, A non-circadian role for clock-genes in sleep homeostasis: A strain comparison. *BMC Neurosci.* **8**, 87 (2007). doi: 10.1186/1471-2202-8-87; pmid: 17945005
29. J. Rizo, C. Rosenmund, Synaptic vesicle fusion. *Nat. Struct. Mol. Biol.* **15**, 665–674 (2008). doi: 10.1038/nsmb.1450; pmid: 18618940
30. E. T. Kavalali, The mechanisms and functions of spontaneous neurotransmitter release. *Nat. Rev. Neurosci.* **16**, 5–16 (2015). doi: 10.1038/nrn3875; pmid: 25524119
31. J. Pratt, C. Winchester, N. Dawson, B. Morris, Advancing schizophrenia drug discovery: Optimizing rodent models to bridge the translational gap. *Nat. Rev. Drug Discov.* **11**, 560–579 (2012). doi: 10.1038/nrd3649; pmid: 22722532
32. S. A. Wolf, A. Melnik, G. Kempermann, Physical exercise increases adult neurogenesis and telomerase activity, and improves behavioral deficits in a mouse model of schizophrenia. *Brain Behav. Immun.* **25**, 971–980 (2011). doi: 10.1016/j.bbi.2010.10.014; pmid: 20970493
33. M. A. Geyer, K. L. McIlwain, R. Paylor, Mouse genetic models for prepulse inhibition: An early review. *Mol. Psychiatry* **7**, 1039–1053 (2002). doi: 10.1038/sj.mp.4001159; pmid: 12476318
34. D. L. Braff, M. A. Geyer, N. R. Swerdlow, Human studies of prepulse inhibition of startle: Normal subjects, patient groups, and pharmacological studies. *Psychopharmacology* **156**, 234–258 (2001). doi: 10.1007/s002130100810; pmid: 11549226
35. A. J. Grottick *et al*., Neurotransmission- and cellular stress-related gene expression associated with prepulse inhibition in mice. *Brain Res. Mol. Brain Res.* **139**, 153–162 (2005). doi: 10.1016/j.molbrainres.2005.05.020; pmid: 15961183
36. S. L. Ameres *et al*., Target RNA-directed trimming and tailing of small silencing RNAs. *Science* **328**, 1534–1539 (2010). doi: 10.1126/science.1187058; pmid: 20558712
37. M. de la Mata *et al*., Potent degradation of neuronal miRNAs induced by highly complementary targets. *EMBO Rep.* **16**, 500–511 (2015). doi: 10.15252/embr.201540078; pmid: 25724380
38. H. Okuno, Regulation and function of immediate-early genes in the brain: Beyond neuronal activity markers. *Neurosci. Res.* **69**, 175–186 (2011). doi: 10.1016/j.neures.2010.12.007; pmid: 21163309
39. S. Bahrami, F. Drabløs, Gene regulation in the immediate-early response process. *Adv. Biol. Regul.* **62**, 37–49 (2016). doi: 10.1016/j.jbior.2016.05.001; pmid: 27220739
40. K. Minatohara, M. Akiyoshi, H. Okuno, Role of immediate-early genes in synaptic plasticity and neuronal ensembles underlying the memory trace. *Front. Mol. Neurosci.* **8**, 78 (2016). pmid: 26778955
41. D. Braff *et al*., Prestimulus effects on human startle reflex in normals and schizophrenics. *Psychophysiology* **15**, 339–343 (1978). doi: 10.1111/j.1469-8986.1978.tb01390.x; pmid: 693742
42. G. M. McAlonan *et al*., Brain anatomy and sensorimotor gating in Asperger's syndrome. *Brain* **125**, 1594–1606 (2002). doi: 10.1093/brain/awf150; pmid: 12077008
43. N. R. Swerdlow, M. A. Geyer, D. L. Braff, Neural circuit regulation of prepulse inhibition of startle in the rat: Current knowledge and future challenges. *Psychopharmacology* **156**, 194–215 (2001). doi: 10.1007/s002130100799; pmid: 11549223
44. M. Latreille *et al*., MicroRNA-7a regulates pancreatic β cell function. *J. Clin. Invest.* **124**, 2722–2735 (2014). doi: 10.1172/JCI73066; pmid: 24789908

ACKNOWLEDGMENTS

We thank all members of the N. Rajewsky laboratory and the C. Birchmeier laboratory for helpful discussions and support. We thank M. Herzog for organizational help, M. Schilling for computational assistance, T. Müller for technical advice on the primary neuronal cultures and discussions, and G. Matz, A. Boltengagen, P. Stallerow, M. Terne, S. Buchert, R. Kabisch, A. Leschke, D. Schreiber, and R. Dannenberg for their technical assistance. L.R.H.-M. acknowledges the European Commission for funding under the scheme Marie Skłodowska-Curie (fellowship 302477). A.R.W. acknowledges funding by Berlin Institute of Health (BIH) grant CRG 2a TP7. S.M. was funded by DFG (German Research Foundation) grant RA 838/6-1. A.F. thanks the DFG Graduate School "Computational Systems Biology" CSB-GRK 1772 for a fellowship and the DZHK (German Centre for Cardiovascular Research) for funding. F.K. and P.G. acknowledge funding from DEEP (Deutsches Epigenom Programm). S.A.W. is supported by DFG grant WO 1418/3-1. C.A.C.J. is funded by the Max Delbrück Center for Molecular Medicine graduate program. L.S. acknowledges funding by DFG grant RA 838/5-1. P.F. is funded by DFG grant SFB/TRR 186 A 04. C.R. acknowledges funding by BIH grant CRG 2b T1. RNA sequencing data are deposited in the Gene Expression Omnibus with accession number GSE93130.

SUPPLEMENTARY MATERIALS

www.sciencemag.org/content/357/6357/eaam8526/suppl/DC1
Materials and Methods
Figs. S1 to S18
Tables S1 to S7
References (*45*–*64*)

25 January 2017; accepted 26 July 2017
Published online 10 August 2017
10.1126/science.aam8526